Mater. Res. Soc. Symp. Proc. Vol. 845 © 2005 Materials Research Society AA5.35

A Hybrid Laser/Aerosol Method for the Synthesis of Porous Nanostructured Calcium Phosphate Materials for Bone Tissue Engineering Applications

Shatoya Brown, Hyunbin Kim, Renato P. Camata
Department of Physics, University of Alabama at Birmingham,
Birmingham, AL 35294, U.S.A.

ABSTRACT

We present a new synthesis method based on laser generation and processing of aerosol particles that can produce calcium phosphate coatings in a porous nanostructured configuration. The process uses laser ablation of crystalline hydroxyapatite targets to produce a calcium phosphate aerosol comprising micro- and nanoparticles that are processed and deposited on metallic substrates under well-controlled temperature and ambient conditions, creating a microporous calcium phosphate network suitable for growth of biogenic calcium phosphate materials. Laser ablation is carried out using a KrF excimer laser at fluences between 0.4 J/cm^2 and 2.8 J/cm^2 and temperatures ranging from 500°C to 760°C. X-ray diffraction and scanning electron microscopy measurements on samples deposited above 750°C show that the obtained material is crystalline hydroxyapatite with good mechanical stability. Its microstructure features a porous framework of partially sintered microparticles surrounded by nanoparticulate material.

INTRODUCTION

Engineering and regeneration of bone tissue remains an outstanding problem in medicine and dentistry [1]. Recent studies show that nanophase materials are promising substrates for bone tissue engineering. Enhanced osteoblast functions have been reported in experiments carried out on nanostructured substrates based on ceramic [2], metallic [3], and carbon-based materials [4]. Nanostructured calcium phosphate bioceramics comprising mixtures of resorbable and nonresorbable calcium phosphate phases are of particular interest in this context because, in addition to their nanoscale morphology, they offer other useful pathways for stimulation of biological activity through their controllable dissolution behavior [5]. Laser methods such as pulsed laser deposition have demonstrated excellent control over the phase composition and microstructure of coatings of these mixtures, establishing them as suitable bioceramic substrates for bone tissue engineering research [6]. In this study we present a novel laser/aerosol method for synthesis of calcium phosphate materials capable of producing coatings with a porous nanostructured configuration. The process may also be scalable for calcium phosphate scaffold fabrication.

Laser ablation of solids in background gases is known to produce particulates with a broad range of sizes and properties [7]. These particulates may form as a result of different energy relaxation mechanisms that take place following laser-solid interactions. Processes as varied as vaporization followed by homogeneous gas phase nucleation and coagulation growth [8], hydrodynamic sputtering [9], and subsurface boiling [10] have been found to play important roles depending on target material and

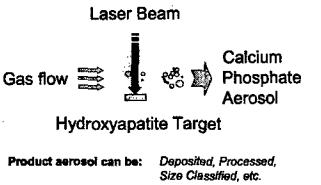

Figure 1. Illustration of how a calcium phosphate aerosol may be generated by laser ablation of a hydroxyapatite ceramic target.

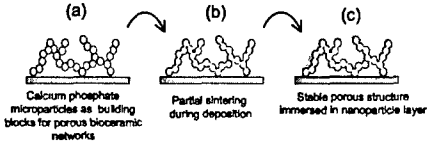

Figure 2. Rationale for the design of a porous nanostructured calcium phosphate substrate to be subjected to cell biology studies aimed at bone tissue engineering.

experimental conditions. Nanoparticle formation is particularly efficient for background pressures in the 0.1-100 kPa range, as the reduced mean free path for vapor species leads to very high collision frequencies and enhanced gas condensation rates. Likewise, these relatively high pressures also lead to very short mean free path for gas-suspended nanoparticles, drastically increasing the time these particles spend in suspension. These two effects significantly reduce the deposition of vapor species and particulate material on nearby surfaces. Although this is highly undesirable for film deposition in conventional pulsed laser deposition arrangements [10], it provides an ideal environment for entraining particulate material in a gas stream. As illustrated in Fig. 1, the particles formed by such a process are entrained in the form of an aerosol (i.e., a suspension of particles in a gas medium) that can be transported to other processing devices and subsequently used as building blocks for new, engineered materials. In this study we have used laser ablation of a hydroxyapatite (HA) [$Ca_{10}(PO_4)_6(OH)_2$] target by the focused beam of a high power pulsed laser in an Ar/H_2O ambient at a pressure of 100 kPa, to generate an aerosol of calcium phosphate particles that can be further processed and used in the production of calcium phosphate-based coatings for tissue engineering studies.

Because of the multiple mechanisms at play during particulate formation, it is typical for particles in very different size regimes to co-exist in aerosols formed during laser ablation [7,11]. It is common, for example, to observe large populations of particles generated by gas phase nucleation and coagulation growth whose sizes range from a few nanometers to tens of nanometers. At the same time, other thermo-mechanical processes (e.g., hydrodynamic sputtering [9]) tend to give rise to much larger particles in the micron size regime. As it will become evident in the following sections, this partition of particulate material in *nanoparticles* and *microparticles* is also observed in the calcium phosphate aerosol formed during ablation of HA. Although these two particle populations are completely intermixed and co-exist in suspension in the same volume, they tend to remain distinct for times up to tens of seconds in the aerosol because of their very different concentrations and gas phase mobilities. They eventually merge into a single mode population due to Brownian coagulation. The goal of the present study was to verify whether the presence of these two sub-populations of very different size could be exploited as a basis to create a new kind of calcium phosphate substrate. The rationale for this process is illustrated in Fig. 2. Calcium phosphate microparticles generated by the laser collide in the gas phase and, upon deposition on a substrate, form fractal aggregates with potentially controllable microporosity [Fig. 2(a)]. High temperatures during flight or after deposition can be adjusted to lead to partial sintering of the microparticles, giving rise to a mechanically stable microporous calcium phosphate framework [Fig. 2(b)]. On the other hand, nanoparticles present in the gas suspension accrete to the microparticles, embedding the microporous network in a nanoparticulate environment [Fig. 3(c)]. In this work we demonstrate the feasibility of synthesizing such porous nanostructured calcium phosphate materials by a laser/aerosol method capable of controlling both nano- and micro- constituents of the resulting material.

EXPERIMENTAL DETAILS

Figure 3 shows a schematic of the laser/aerosol apparatus employed for the synthesis of porous nanostructured calcium phosphates. An equilibrium Ar/H_2O gas mixture obtained by

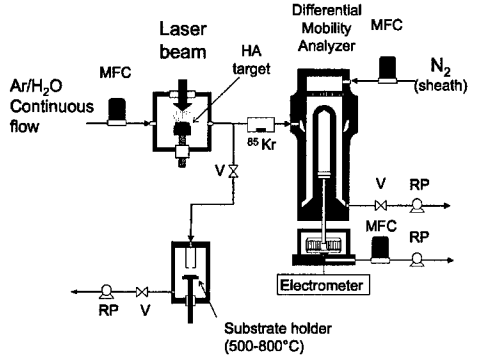

Figure 3. Schematic of laser/aerosol apparatus used for deposition of calcium phosphates. The system includes a differential mobility analyzer that can be used for on-line determination of size distributions of the gas-suspended nanoparticles (MFC, V, and RP stand for Mass Flow Controller, Valve, and Rotary Pump).

bubbling Ar gas (99.9995% purity) through deionized water kept just below the boiling point is flowed into a sealed chamber containing a solid target prepared by compressing a commercial HA powder (97.5 % purity, Plasma Biotal Ltd.) at a pressure of 2500 psi and sintered at 1200 °C in Ar/H_2O atmosphere for 1.5 hrs. The target, in the shape of a flat disk, is mounted on a holder coupled to a variable speed motor enabling continuous target rotation during experiments. A calcium phosphate aerosol is obtained by the ablation of this HA target at a pressure of 100 kPa using the focused beam of a KrF excimer laser (248 nm). The product aerosol is then directed to a deposition chamber and deposited by inertial impaction [12] on polished Ti-6Al-4V substrates mounted on a rotating substrate holder heated to temperatures in the 500-800°C range. Alternatively, the aerosol particles formed in the laser ablation chamber may also be deflected to an adjacent chamber containing a sealed ^{85}Kr radioactive source that ionizes the carrier gas and imparts an equilibrium charge distribution to the calcium phosphate aerosol [13]. This aerosol now possessing a well-known charge distribution is introduced into a system featuring a differential mobility analyzer and an aerosol electrometer whose combined operation allows the on-line measurement of the size distribution of the calcium phosphate aerosol in the 1-100 nm range. The use of this approach for on-line spectrometry of gas-suspended nanoparticles has been described in detail elsewhere [7]. Briefly, the differential mobility analyzer is an aerodynamic analog of a dispersive mass spectrometer. It consists of a coaxial capacitor in which charged particles migrate across a particle-free laminar sheath gas flow due to an applied electric field. Particles with different sizes will move along different trajectories as a result of their different aerodynamic drag. This enables the separation of particles according to size. The analyzer used in our experiments features inner and outer electrodes with diameters of 25 and 32 mm, respectively, and a classification region with a length of 18 mm [14]. The instrument was operated with an aerosol flow rate of 1 SLM (standard liter per minute) of Ar/H_2O and 5 SLM of N_2 sheath gas, allowing measurements of the aerosol size distribution in the 1-80 nm range. Flow rates were maintained constant through the use of mass flow controllers. Inversion of the mobility data to yield the actual size distributions was based on standard equilibrium charge distributions calculated according to Fuchs theory [13,14]. Measurements were performed for laser fluences on the HA target surface between 0.4 and 2.8 J/cm^2 where the laser beam was focused to a spot with an area of 0.02 cm^2.

RESULTS AND DISCUSSION

Effect of substrate temperature on resulting calcium phosphate

Previous studies on the use of high power pulsed lasers for the production of calcium phosphate coatings have shown that laser ablation tends to cause the dehydroxylation of HA,

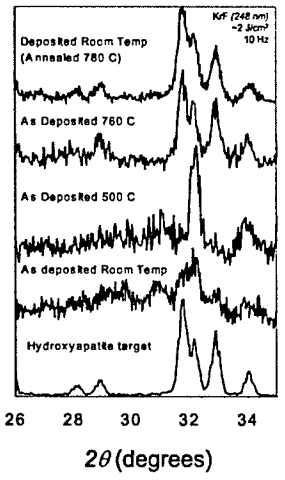

Figure 4. X-ray diffraction scans of calcium phosphate layers deposited by the described laser/aerosol method at various substrate temperatures.

leading to the formation of coatings dominated by tricalcium phosphate or tetracalcium phosphate [6]. Two experimental parameters have proven critical to control this effect, namely, the water content of the background atmosphere (typically controlled by varying the pressure in the deposition chamber) and the substrate temperature. Water availability in the background environment of the laser plume is a necessary but not sufficient condition to produce crystalline HA coatings. A high enough substrate temperature must be used to ensure the incorporation of hydroxyl groups in the coating. Figure 4 shows that this effect is also observed in the material produced through our laser/aerosol process. Samples deposited with substrate kept at room temperature show a material with lack of long-range order, possibly comprised of small crystallites surrounded by amorphous material. Deposition at 500°C produces a material with a strong reflection ascribed to calcium oxide, while deposition above 760°C leads to crystalline HA. Crystalline HA may also be obtained by annealing of samples deposited at room temperature. Figure 5 shows scanning electron microscopy images of the calcium phosphate deposited at 760°C, which the X-ray diffraction data establishes to be crystalline HA. The microstructure of the material produced at 760°C as revealed by scanning electron microscopy (Fig. 5), shows a network of partially sintered microparticles with sizes in the 0.5 – 2.0 μm range. Figure 5(c), in particular, indicates that the microparticles are surrounded by smaller objects with sizes below 100 nm, which suggests that our original intent of producing a micronetwork embedded in nanophase material has been at least partially achieved.

Size distributions of calcium phosphate aerosol

The rationale explored in this work for fabrication of porous nanostructured calcium phosphate substrates (Fig. 2) relies on the ability to control the original aerosol size distribution produced by the laser ablation process. In an attempt to achieve a high level of control over the aerosol population that leads to our coatings, we have conducted direct measurements on the gas-

(a) (b) (c)

Figure 5. Scanning electron microscopy images of a hydroxyapatite layer deposited by the described laser/aerosol method at a substrate temperature of 760 °C. (Same sample at three different magnifications.)

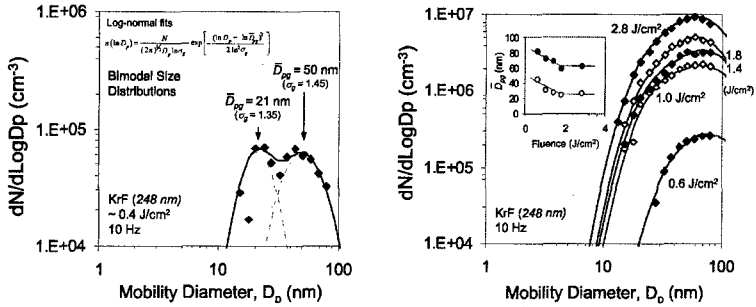

Figure 6. Size distributions of calcium phosphate aerosol generated during laser ablation of hydroxyapatite target at various laser fluences.

suspended particle population prior to deposition using the differential mobility analyzer/electrometer system described in the previous section. Figure 6 shows the size distributions obtained for various laser fluences. In Fig. 6(a) the size distribution measured for an energy density of ~0.4 J/cm^2 is shown. This energy density corresponds to the lowest fluence for which particles can be detected in our system. The concentrations obtained as a function of size are strongly suggestive of a bimodal size distribution. The measured distribution can be approximately reproduced by the superposition of two log-normal distributions centered around 21 nm and 50 nm respectively. The geometric standard deviation for these distributions are very close to $\sigma_g = 1.4$, which is typical of aerosols formed by Brownian coagulation [15]. Figure 6(b) shows distributions obtained at increasingly higher laser energy densities. Although a cursory inspection of these distributions may suggest single mode distributions, each data set is again best fitted by the superposition of two log-normal functions whose geometrical mean, D_{pg}, varies with laser energy density. The inset in Fig. 6(b) shows that D_{pg} for both distributions shifts to lower values as the laser energy density increases. The value of D_{pg} for the first distribution spans the 20-40 nm range whereas the second distribution varies between 50 and 80 nm. The number concentration associated with these two distributions is also significantly different. Table I summarizes the total number of particles associated with each of the log-normal functions fitted to the data. For the range of energy densities explored, the number concentration of the particle distribution centered around 50-80 nm (i.e., N_2) is greater than the concentration of particles in the 20-40 nm range (i.e., N_1) by factors between 4 and 10. One possible explanation for the bimodal nature of this size distribution is the flow characteristics of our ablation chamber. The observed bimodal distribution may result from a fractionation of the original aerosol population into a fast traveling set of nanoparticles that moves rapidly from the point where they are generated to the point of measurement (i.e., differential mobility analyzer) and a slower set of particles that remains trapped in the ablation chamber and, as a result, has time to grow by collisions resulting from Browning motion. This suggests that a redesign of our ablation chamber may be necessary to

Table I. Total concentrations of aerosol particles in the two modes of the calcium phosphate size distribution.

J/cm²	N_1 (10⁴ cm⁻³)	N_2 (10⁴ cm⁻³)
0.6	1.0	6.00
1.0	15	50.0
1.4	17	80.0
1.8	12	120
2.8	41	220

better control this nanoparticle population and enable its more controllable use as the source of nanophase medium for potential biological stimulation in our coatings.

Because of the limited dynamic range of the differential mobility analyzer (1-100 nm), it was not possible to ascertain from direct aerosol measurements the concentration of the much larger microparticles (0.5-2 μm) that must also be present in the aerosol and that lead to the micro-framework observed in our scanning electron microscopy images. On-going work in our laboratory is focused on probing the effects of ablation and deposition conditions on the characteristics of this microparticle network.

CONCLUSIONS

KrF excimer laser ablation of crystalline HA was used to generate a calcium phosphate aerosol that was deposited on Ti-6Al-4V substrates. Fluences between 0.4 and 2.8 J/cm^2 with deposition temperatures between room temperature and 760°C were utilized. For deposition above 750°C, adhesion, X-ray diffraction and scanning electron microscopy analyses show that samples are crystalline HA with microporous morphology resulting from partial sintering of microparticles in a nanoparticulate environment. Such samples exhibit good mechanical stability. Direct measurements on calcium phosphate nanoparticle aerosol used in the synthesis reveal bimodal log-normal size distributions with concentration features in two different size regimes at the nanoscale, namely, at 20-40 nm and at 50-80 nm. Our results suggest that further manipulation of experimental parameters involved in this novel synthesis method may enable control of pore size, micro-framework stability, nanoparticle size and concentration, and perhaps even crystalline phase make-up of calcium phosphate substrates for tissue engineering studies.

ACKNOWLEDGEMENTS

We acknowledge support from the Research Experiences for Undergraduates (REU) program funded by the NASA-Alabama Space Grant Consortium at the UAB campus. Instrumentation for this research was supported by the National Science Foundation (NSF) under grant DMR-0116098 (Major Research Instrumentation). Special thanks to Masashi Matsumura and Cheri Moss for assistance with aerosol mobility measurements and electron microscopy, respectively.

REFERENCES

1. Y. Yamada, M. Ueda, T. Naiki, M. Takahashi, K.-I. Hata, and T. Nagasaka, *Tissue Eng.* **10**, 955 (2004).
2. T. J. Webster, C. Ergun, R. H. Doremus, R. W. Siegel, and R. Bizios, *Biomaterials* **21**, 1803 (2000).
3. T. J. Webster and J. U. Ejiofor, *Biomaterials* **25**, 4731 (2004).
4. R. L. Price, K. Ellison, K.M. Haberstroh, T. J. Webster, *J. Biomed. Mater. Res.* **70**, 129 (2004).
5. H. Kim, Y. K. Vohra, P. J. Louis, W. R. Lacefield, J.E. Lemons, and R. P. Camata, *Key Eng. Mater.* **284-286**, 207 (2005).
6. H. Kim, Y. K. Vohra, R. P. Camata, and W. R. Lacefield, *J. Mater. Sci. Mater. Med., in press.*
7. R. P. Camata, M. Hirasawa, K. Okuyama, and K. Takeuchi, *J. Aerosol Sci.* **31**, 391 (2000).
8. T. Makimura, Y. Kunii, and K. Murakami, *Jpn. J. Appl. Phys.* **35**, 4780 (1996).
9. R. Kelly and A. Miotello, "Mechanisms of pulsed laser sputtering," *Pulsed Laser Deposition of Thin Films*, ed. D. B. Chrisey and G. K. Hubler (Wiley, 1994) pp. 55-87.
10. J.T. Cheung, "History and fundamentals of pulsed laser deposition," *Pulsed Laser Deposition of Thin Films*, ed. D. B. Chrisey and G. K. Hubler (Wiley, 1994) pp. 14-15.
11. W. T. Nichols, G. Malyavanatham, D. E. Henneke, D.T. O'Brien, M.F. Becker, and J.W. Keto, *J. Nanopart. Res.* **4**, 423 (2002).
12. J. Fernández de la Mora, S. V. Hering, N. Rao, and P. H. McMurry, *J. Aerosol Sci.* **21**, 169 (1990).
13. N.A. Fuchs, *Geofis. Pura Appl.* **56**, 185 (1963).
14. T. Seto, T. Nakamoto, K. Okuyama, M. Adachi, Y. Kuga, and K. Takeuchi, *J. Aerosol Sci.* **28**, 193 (1997).
15. J. H. Seinfeld, "Atmospheric Chemistry and Physics of Air Pollution," (Wiley, 1986).